

# Study of pool boiling and critical heat flux enhancement in nanofluids

S.J. KIM, I.C. BANG, J. BUONGIORNO\*, and L.W. HU

Massachusetts Institute of Technology, 77 Massachusetts Avenue, Cambridge, 02139-4307 MA, USA

**Abstract.** The pool boiling characteristics of dilute dispersions of alumina, zirconia and silica nanoparticles in water were studied. These dispersions are known as nanofluids. Consistently with other nanofluid studies, it was found that a significant enhancement in Critical Heat Flux (CHF) can be achieved at modest nanoparticle concentrations ( $<0.1\%$  by volume). Buildup of a porous layer of nanoparticles on the heater surface occurred during nucleate boiling. This layer significantly improves the surface wettability, as shown by a reduction of the static contact angle on the nanofluid-boiled surfaces compared with the pure-water-boiled surfaces. CHF theories support the nexus between CHF enhancement and surface wettability changes. This represents a first important step towards identification of a plausible mechanism for boiling CHF enhancement in nanofluids.

**Key words:** nanofluids, nanoparticle deposition, critical heat flux, pool boiling, wettability, contact angle.

## 1. Introduction

Addition of solid nanoparticles to common fluids such as water is an effective way to increase the Critical Heat Flux (CHF). The resulting colloidal suspensions are known in the literature as nanofluids. Materials used for nanoparticles include noble metals (e.g., gold, silver, platinum) and metal oxides (e.g., alumina, zirconia, silica, titania). Previous studies of CHF in nanofluids [1–6] have established that:

1. Significant CHF enhancement (up to 200%) occurs with various nanoparticle materials, e.g., silicon, aluminum and titanium oxides.
2. Such enhancement occurs at low nanoparticle concentrations, typically less than 1% by volume.
3. During nucleate boiling some nanoparticles precipitate on the surface and form a porous layer.

At MIT we are conducting research to assess the feasibility of water-based nanofluids for nuclear reactors [7]. The work includes single-phase heat transfer, thermo-physical properties measurements, characterization of pool boiling CHF and flow boiling CHF mechanisms. In theory nanofluids can improve the thermal performance of any engineering system that is limited by CHF. To explore the CHF enhancement mechanism of nanofluids, we conducted pool boiling experiments with both wire and flat heaters. Our findings are outlined in this paper. Experimental results and their interpretation are summarized in Sections 2 and 3, respectively.

## 2. Pool boiling CHF experiments

**2.1. Preparation and characterization of nanofluids.** Three nanoparticle materials, i.e. alumina ( $\text{Al}_2\text{O}_3$ ), zirconia ( $\text{ZrO}_2$ ) and silica ( $\text{SiO}_2$ ), were selected for the

experiments. Water-based nanofluids of these three materials were purchased from Sigma-Aldrich (alumina and zirconia) and Applied Nanoworks (silica). The vendor-specified concentration of the nanofluids was 10% by weight. The as-purchased nanofluids were then diluted with deionized water to the low concentrations of interest for the CHF experiments, i.e., 0.001, 0.01 and 0.1% by volume. The size (effective diameter) of the nanoparticles in the dilute nanofluids was measured with the dynamic light scattering technique and ranged from 110 to 210 nm for alumina nanofluids, 110 to 250 nm for zirconia nanofluids, and 20 to 40 nm for silica nanofluids. Various parameters relevant to two-phase heat transfer were also measured or estimated. First, the boiling point of the dilute nanofluids was measured with a thermocouple and found to be within  $\pm 1^\circ\text{C}$  of pure water. The surface tension, thermal conductivity and viscosity of the nanofluids were measured by means of a tensometer, a thermal conductivity probe and a capillary viscometer, respectively. These properties were found to differ negligibly from those of pure water, i.e., within  $\pm 5\%$ . At the low concentration of interest, also the fluid density and the heat of vaporization can be considered unchanged. In summary, the transport and thermodynamic properties of the dilute nanofluids used in our experiments are very similar to those of pure water.

**2.2. CHF experiments with wires.** The CHF of deionized pure water and nanofluids was measured with a wire heater horizontally submerged in the test fluid at atmospheric pressure, surrounded by an isothermal bath. The experimental apparatus and procedure were described in a previous paper [6]. Measured CHF values are shown in Fig. 1. Significant CHF enhancement is observed for all nanofluids, up to 52% with alumina nanofluids, up

\*e-mail: jacopo@mit.edu

to 75% with zirconia nanofluids and up to 80% for silica nanofluids. The CHF dependence on nanoparticle concentration is erratic, but not unprecedented for nanofluids [3].

on boiling heat transfer through changes in roughness and wettability, as explained in the following sections.

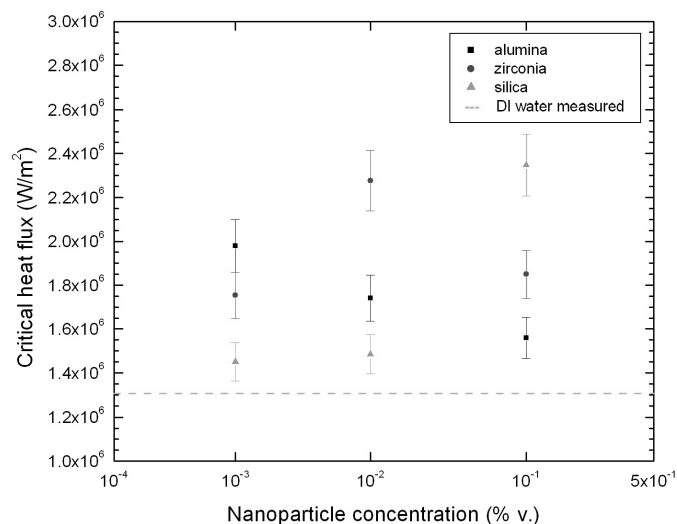


Fig. 1. CHF data for pure water and alumina, zirconia and silica nanofluids

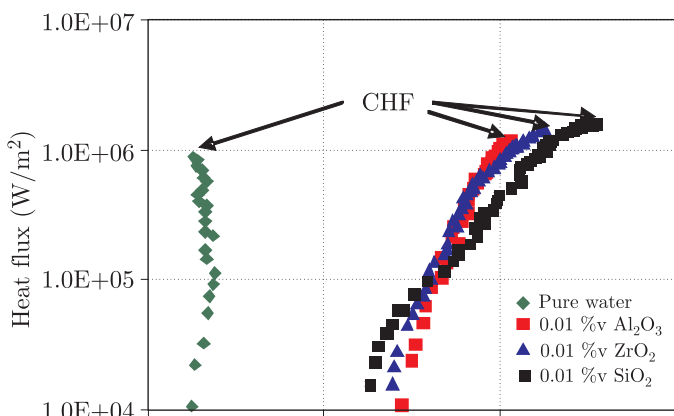


Fig. 2. Boiling curves for stainless steel wire (Uncertainties in the slope of the resistivity-temperature curve for stainless steel and the non-negligible temperature drop within the wire contribute to the unusually high values of the superheat in this boiling curve)

Typical boiling curves for pure water and two nanofluids are shown in Fig. 2. Note that the nanofluids have higher CHF, but lower nucleate boiling heat transfer coefficient, which is consistent with the findings of Das et al. [8] and Bang and Chang [3]. The deterioration of nucleate boiling suggests that a surface effect is at work. Scanning Electron Microscope (SEM) analysis of the wire surface reveals that the surface is clean during pure water boiling (Fig. 3a), but a porous layer builds up during nanofluid boiling (Fig. 3b). We believe this layer is due to boiling-induced precipitation of some nanoparticles. Energy Dispersive Spectrometer (EDS) analysis of the layer confirms that it is made of nanoparticle material. The presence of a porous layer on the surface undoubtedly has an impact

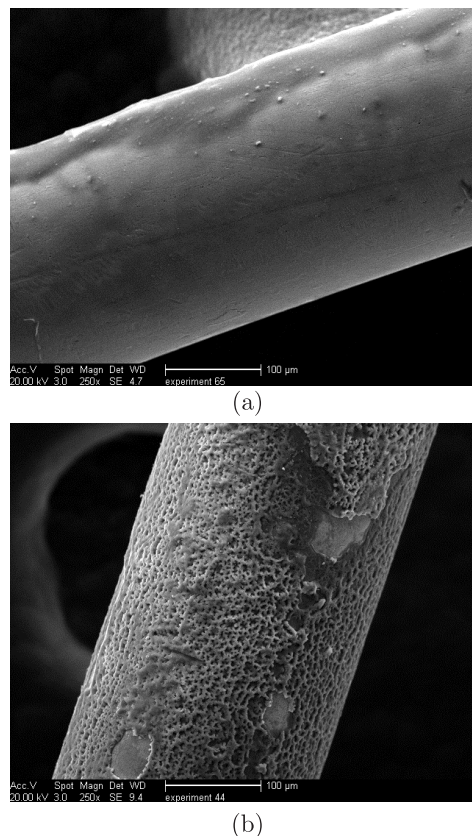


Fig. 3. SEM images of steel wires taken after boiling pure water and 0.01 v% alumina nanofluid

**2.3. Flat heater experiments.** Use of a thin wire heater is convenient for CHF experiments, but its high curvature makes it inconvenient for surface analysis, such as required to study the porous layer. For this purpose we switched to flat plates, 5 mm wide, 45 mm long, 0.05 mm thick, made of stainless steel grade 316. Using the same apparatus, several flat heaters were boiled in nanofluids for a period of 5 minutes and at a heat flux of 500 kW/m<sup>2</sup>. The SEM and EDS analyses again revealed that some nanoparticles precipitate on the heater surface and form irregular porous structures, which do not appear during boiling of pure water (Fig. 4).

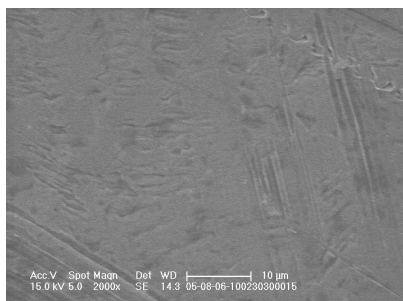
An important effect caused by the porous layer is the increase in surface wettability. The static contact angle,  $\theta$ , was measured for sessile droplets of pure water and nanofluids at 22°C in air on the clean and nanoparticle-fouled surfaces boiled in nanofluids. The uncertainty on such measurements is estimated to be  $\pm 10^\circ$ . Low values of the contact angle correspond to high surface wettability. A few representative cases are shown in Fig. 5. The complete contact angle database is reported in Table 1. A rather dramatic decrease of the contact angle on the fouled surfaces is evident. Such decrease occurs with pure water as well as nanofluid droplets, thus suggesting that wettability is enhanced by the porous layer on the surface, not the nanoparticles in the fluid.

Table 1

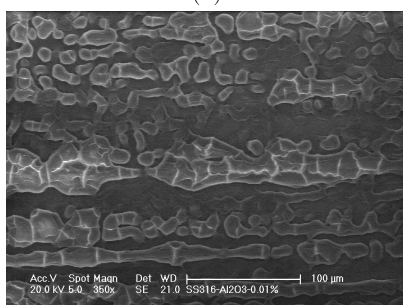
Static contact angles for water and nanofluids on clean and fouled surfaces

Fluid	Pure water	Al <sub>2</sub> O <sub>3</sub> nanofluid			ZrO <sub>2</sub> nanofluid			SiO <sub>2</sub> nanofluid		
Nanoparticle concentration (%v)	0	0.001	0.01	0.1	0.001	0.01	0.1	0.001	0.01	0.1
Clean surface	79°	80°	73°	71°	80°	80°	79°	71°	80°	75°
Nanofluid boiled surface	8°–36° <sup>a</sup>	14°	23°	40°	43°	26°	30°	11°	15°	21°

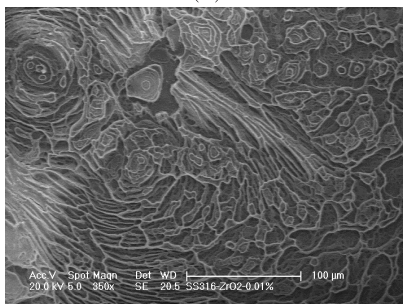
<sup>a</sup>22°–30° on surfaces boiled in alumina nanofluids, 16°–36° on surfaces boiled in zirconia nanofluids, 8°–18° on surfaces boiled in silica nanofluids



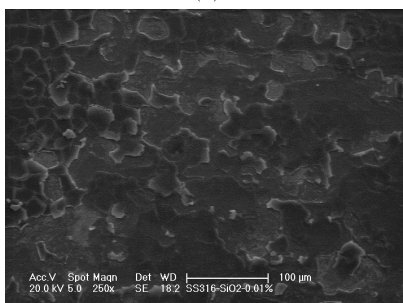
(a)



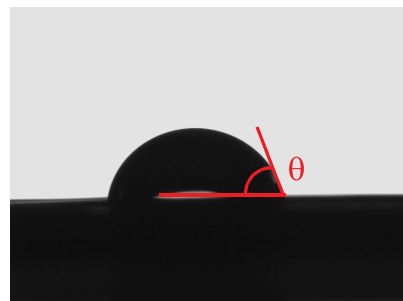
(b)



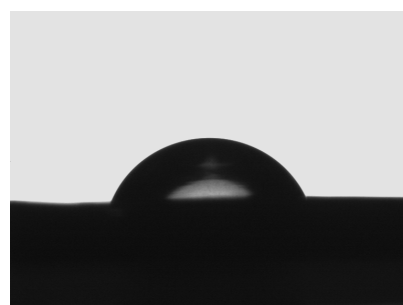
(c)



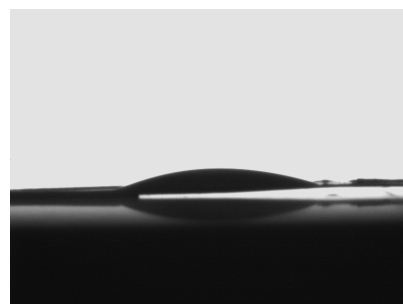
(d)



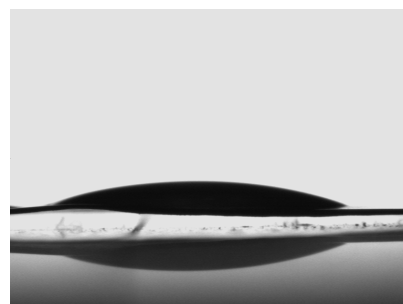
(a)  $\theta = 79^\circ$



(b)  $\theta = 73^\circ$



(c)  $\theta = 22^\circ$



(d)  $\theta = 23^\circ$

Fig. 4. SEM images of flat heater surface boiled in (a) pure water, (b) 0.01 v% alumina nanofluid, (c) 0.01 v% zirconia nanofluid, (d) 0.01 v% silica nanofluid. Similar structures were observed at the other concentrations tested in this study

Fig. 5. Static contact angles of 5- $\mu$ L sessile droplets on stainless steel surfaces, measured with a Krüss goniometer equipped with a camera monitor. (a) Pure water droplet on surface boiled in pure water, (b) 0.01 v% alumina nanofluid droplet on surface boiled in pure water; (c) pure water droplet on

surface boiled in 0.01 v% alumina nanofluid, (d) 0.01v% alumina nanofluid droplet on surface boiled in 0.01 v% alumina nanofluid. Qualitatively similar results were obtained for silica and zirconia nanofluids at all the concentrations tested in our experiments

### 3. Data interpretation

The experiments presented in Section 2 have shown that nanofluids exhibit enhanced CHF at low nanoparticle concentrations, that during nanofluid boiling the heater surface becomes coated with a porous layer of nanoparticles, and that such layer significantly increases surface wettability. In this section we address two key questions related to the above observations. Why do the nanoparticles precipitate? What effect does the nanoparticle layer have on nucleate boiling and CHF?

#### 3.1. Why the nanoparticles deposit on the surface during nucleate boiling.

We have observed no significant deposition of nanoparticles while handling nanofluids or measuring their properties or even in single-phase convective heat transfer experiments, which are being run in our lab. Thus, we concluded that development of the nanoparticle layer is a direct consequence of boiling, but what is the mechanism of nanoparticle deposition on the surface during nucleate boiling? It is well known that a thin liquid microlayer develops underneath a vapor bubble growing at a solid surface [9]. Microlayer evaporation with subsequent settlement of the nanoparticles initially contained in it could be the reason for the formation of the porous layer. To verify the plausibility of this hypothesis, we make use of the following simple model. The volume of nanoparticles contained in the liquid microlayer is  $\delta_m \frac{\pi}{4} D_b^2 \varphi$ , where  $\delta_m$  is the thickness of the microlayer,  $D_b$  is the bubble departure diameter and  $\varphi$  is the nanoparticle volume fraction in the nanofluid. The number of bubbles generated per unit time and surface area is  $n'' f_b$ , where  $n''$  is the active nucleation site density and  $f_b$  is the bubble departure frequency. Then the rate of growth of the nanoparticle layer on the surface,  $\dot{\delta}$ , is:

$$\dot{\delta} \sim \delta_m \frac{\pi}{4} D_b^2 \varphi n'' f_b. \quad (1)$$

The active nucleation site density can be estimated from the energy balance at the surface as

$$n'' \sim q'' / \left( \frac{\pi}{6} D_b^3 \rho_g h_{fg} f_b \right),$$

where  $q''$  is the heat flux (500 kW/m<sup>2</sup> in our case). Substituting this expression into Eq. (1), we get:

$$\dot{\delta} \sim \frac{3}{2} \frac{\delta_m \varphi q''}{D_b \rho_g h_{fg}}. \quad (2)$$

The bubble departure diameter for water at atmospheric pressure can be estimated from the Cole and Rosenhow's correlation [10], which gives  $D_b \sim 2.4$  mm. Assuming also  $\delta_m \sim 1$   $\mu$ m, as recommended by Collier and Thome [9] for

water at atmospheric pressure, we find  $\dot{\delta} \sim 0.02$   $\mu$ m/sec for  $\varphi = 10^{-4}$ . The duration of the experiments with the flat heaters is approximately 5 minutes, resulting in a thickness of the nanoparticle layer of about 6  $\mu$ m, which is the same order of magnitude of the structures observed with the SEM and profilometer. Given the uncertainties in the model parameters (especially the values of  $D_b$  and  $\delta_m$ ), the agreement is deemed acceptable.

#### 3.2. Effect of nanoparticles on nucleate boiling.

The most remarkable characteristic of nucleate boiling in our nanofluid experiments was the reduction of the heat transfer coefficient, as revealed by the boiling curve shift to the right (Fig. 2). It is interesting to note that heat transfer deterioration in the nucleate boiling regime was also observed by Das et al. [8] and Bang and Chang [3]. On the other hand, heat transfer enhancement was reported by Dinh et al. [11] and Wen and Ding [12], while You et al. [1] and Vassallo et al. [2] reported no change of heat transfer in the nucleate boiling regime. Wen and Ding [12] proposed that these conflicting trends could be due to poorly characterized/reported factors such as initial surface roughness, presence of surfactants, agglomeration of particles, surface contamination, etc. A way to capture some of these effects is to consider Wang and Dhir's [13] expression for the nucleation site density:

$$n'' \propto N_c (1 - \cos \theta) (T_w - T_{sat})^6, \quad (3)$$

where  $N_c$  is the number of microcavities per unit surface area and  $T_w - T_{sat}$  is the wall superheat.

According to Eq. (3) a decrease of the contact angle would tend to decrease the active nucleation site density and thus the heat transfer coefficient. However, nanoparticle deposition also alters the surface roughness and number of microcavities present on the surface. In our boiling experiments with stainless steel wire heaters submerged in nanofluids containing metal oxide nanoparticles the number of microcavities and the surface roughness are typically increased (Figs. 3 and 4), which is in agreement with the findings in reference [3]. However, other researchers have reported a decrease in surface roughness upon nanofluid boiling [8]. This apparent discrepancy could be due to differences in the nanoparticle size, initial morphology of the substrate surface, particle deposition rate, and duration of the experiment. For example, deposition of small particles on surfaces with relatively large cavities could lead to filling the cavities, and thus reduce roughness; vice versa, deposition of large particles on an initially smooth surface will lead to higher surface roughness. However, lacking direct measurement of the nucleation site density, the link between boiling curve shift and nanoparticle layer cannot be conclusively elucidated. Clearly, this is an area that warrants additional study.

**3.3. Effect of nanoparticles on CHF.** The literature is generally deficient in explaining the CHF enhancement mechanism in nanofluids. Despite several decades of in-

tense study a consensus explanation of the physical mechanism causing CHF is yet to be found even for the simpler case of a pure substance. Hypotheses have been formulated, most of which generally fall into one of four categories: hydrodynamic instability theory [14,15], macro-layer dryout theory [16–18], hot/dry spot theory [19], and bubble interaction theory [20,21]. Of these four theories, the last three support surface wettability in relation to CHF enhancement. A thorough review of these theories is presented in reference [22]. To illustrate the effect of surface wettability on CHF, a review of the hot/dry spot theory is given below.

If the heat flux is high, hot/dry spots develop within the bases of the bubbles growing at certain nucleation sites. The hot/dry spots can be reversible or irreversible. They are reversible if rewetting occurs upon bubble departure. They are irreversible if rewetting does not occur, which causes a runaway excursion of the surface temperature and eventually burnout [19]. In principle the presence of the nanoparticle layer on the surface can help delay CHF in two ways. First, its increased wettability promotes rewetting upon bubble departure. Second, the layer may assist in dissipating the hot spot by enhancing radial conduction on the surface. The latter effect is small, as the thickness of the nanoparticle layer is of the order of a few microns. To assess the importance of the wettability effect, we can avail ourselves of the model proposed by Theofanous and Dinh [23], who considered the microhydrodynamics of the solid-liquid-vapor line at the boundary of a hot/dry spot. They postulate that CHF occurs when the evaporation recoil force, which drives the liquid meniscus to recede, becomes larger than the surface tension force, which drives the meniscus to advance and rewet the hot/dry spot. On this basis, they derived the following expression for the CHF:

$$q''_{cr} = \kappa^{-1/2} \rho_g h_{fg} \left[ \frac{\sigma(\rho_f - \rho_g)g}{\rho_g^2} \right]^{1/4}. \quad (4)$$

Note that Eq. (4) and the traditional Kutateladze-Zuber's formula [14,15] are essentially the same, except for the parameter  $\kappa$ , which is the coefficient of proportionality between the radius of curvature of the liquid meniscus,  $\mathfrak{R}$ , and the capillary length:

$$\mathfrak{R} = \kappa \sqrt{\frac{\sigma}{g(\rho_f - \rho_g)}}. \quad (5)$$

Theofanous and Dinh [23] state that  $\kappa$  is a surface-dependent parameter that 'for a well-wetting surface is smaller than for a poorly-wetting surface', however they do not provide an analytical expression for it. Using elementary geometry and Lord Rayleigh's formula for the volume of a static liquid meniscus [24], the average radius of curvature of the meniscus can be evaluated as:

$$\mathfrak{R} = \sqrt{\frac{\sigma}{g(\rho_f - \rho_g)}} / \sqrt{1 - \frac{\sin \theta}{2} - \frac{\pi/2 - \theta}{2 \cos \theta}}. \quad (6)$$

Comparing Eqs. (5) and (6), we can get an expression

for  $\kappa$ :

$$\kappa = \left( 1 - \frac{\sin \theta}{2} - \frac{\pi/2 - \theta}{2 \cos \theta} \right)^{-1/2}. \quad (7)$$

The values of  $\kappa$  for  $\theta \sim 70^\circ$  (clean surface) and  $\theta \sim 20^\circ$  (nanoparticle-fouled surface) are about 7.10 and 2.36, respectively, thus Eq. (4) suggests that the CHF would increase by a factor  $\sqrt{7.10/2.36} \sim 1.73$  or 73%. This estimate is remarkably close to the CHF enhancement observed in our experiments. In summary, the hot/dry spot theory seems to corroborate the link between increased surface wettability and CHF enhancement in nanofluids.

## 4. Conclusions and future work

The main findings of this study are as follows:

- Dilute dispersions of alumina, zirconia and silica nanoparticles in water exhibit significant CHF enhancement in boiling experiments with wire heaters.
- During nucleate boiling some nanoparticles deposit on the heater surface to form a porous layer. This layer improves the wettability of the surface considerably, as measured by a marked reduction of the static contact angle.
- The higher wettability can produce CHF enhancement which is consistent in magnitude with the experimental observations.

To elucidate CHF enhancement mechanism more definitively, additional work is however needed, including a thorough characterization of the layer growth and morphology during boiling, which will clarify the effect of the porous layer on the nucleation site density.

## REFERENCES

- [1] S.M. You, J. Kim, and K.H. Kim, "Effect of nanoparticles on critical heat flux of water in pool boiling heat transfer", *Applied Physics Letters* 83 (16), 3374–3376 (2003).
- [2] P. Vassallo, R. Kumar, and S.D'Amico, "Pool boiling heat transfer experiments in silica-water nano-fluids", *Int. J. Heat and Mass Transfer* 47, 407–411 (2004).
- [3] I. C. Bang and S. H. Chang, "Boiling heat transfer performance and phenomena of Al<sub>2</sub>O<sub>3</sub>-water nano-fluids from a plain surface in a pool", *Int. J. Heat and Mass Transfer* 48, 2407–2419 (2005).
- [4] D. Milanova and R. Kumar, "Role of ions in pool boiling heat transfer of pure and silica nanofluids", *Applied Physics Letters* 87, 233107 (2005).
- [5] H. Kim, J. Kim, and M. Kim, "Experimental study on CHF characteristics of water-TiO<sub>2</sub> nano-fluids", *Nuclear Engineering and Technology* 38 (1), 2006.
- [6] S.J. Kim, B. Truong, J. Buongiorno, L.W. Hu, and I.C. Bang, "Study of two-phase heat transfer in nanofluids for nuclear applications", *Proc. ICAPP '06*, USA, paper 6005 (2006).
- [7] J. Buongiorno and L.-W. Hu, "Nanofluid coolants for advanced nuclear power plants", *Proc. ICAPP '05*, paper 5705 (2005).

- [8] S. Das, N. Putra, and W. Roetzel, "Pool boiling characteristics of nano-fluids", *Int. J. Heat and Mass Transfer* 46, 851–862 (2003).
- [9] J.G. Collier and J.R. Thome, *Convective Boiling and Condensation*, 3<sup>rd</sup> ed., Science Publications, Oxford, 1996.
- [10] R. Cole and W. Rosenhow, "Correlation of bubble departure diameters for boiling of saturated liquids", *Chem. Eng. Prog. Symp. Ser.* 65 (92), 211–213 (1969).
- [11] T.N. Dinh, J.P. Thu, and T.G. Theofanous, "Burnout in high heat flux boiling: the hydrodynamic and physico-chemical factors", 4<sup>2<sup>nd</sup></sup> *AIAA Aerospace Sciences Meeting and Exhibit*, Nevada, 2004.
- [12] D. Wen and Y. Ding, "Experimental investigation into the pool boiling heat transfer of aqueous based  $\gamma$ -alumina nanofluids", *J. Nanoparticle Research* 7, 265–274 (2005).
- [13] C.H. Wang and V.K. Dhir, "Effect of surface wettability on active nucleation site density during pool boiling of water on a vertical surface", *J. Heat Transfer* 115, 659–669 (1993).
- [14] S.S. Kutateladze, "Heat transfer in condensation and boiling", *AEC-TR-3770* (1952).
- [15] N. Zuber, "Hydrodynamic aspects of boiling heat transfer", *AECU-4439* (1959).
- [16] Y. Haramura and Y. Katto, "A new hydrodynamic model of CHF applicable widely to both pool and forced convection boiling on submerged bodies in saturated liquids", *Int. J. Heat and Mass Transfer* 26, 389–399 (1983).
- [17] P. Sadasivan, P.R. Chappidi, C. Unal, and R.A. Nelson, "Possible mechanisms of macrolayer formation", *Pool and External Flow Boiling (ASME 1992)*, 135 (1992).
- [18] Y. Katto and S. Yokoya, "Principal mechanism of boiling crisis in pool boiling", *Int. J. Heat and Mass Transfer* 11, 993–1002 (1968).
- [19] T.G. Theofanus et al., "The boiling crisis phenomenon. Part II: dryout dynamics and burnout", *Experimental Thermal and Fluid Science* 26, 793–810 (2002).
- [20] W. Rosenhow and P. Griffith, "Correlation of maximum heat flux data for boiling of saturated liquids", *Chem. Eng. Prog. Symp. Ser.* 52 (18), 47–49 (1956).
- [21] N. Kolev, "How accurately can we predict nucleate boiling?", in *Multiphase Flow Dynamics 2*, Springer, Berlin, 2002.
- [22] S. Kim, I.C. Bang, J. Buongiorno and L.-W. Hu, "Surface wettability change during pool boiling of nanofluids and its effect on critical heat flux", *Int. J. Heat and Mass Transfer* (2007), (to be published).
- [23] S.J. Kim, I.C. Bang, J. Buongiorno, and L.W. Hu, "Surface wettability change during pool boiling of nanofluids and its effect on critical heat flux", *Int. J. Heat and Mass Transfer* 50, 4105–4116 (2007).
- [24] S.V. Gupta, "Capillary action in narrow and wide tubes – a unified approach", *Metrology* 41, 361–364 (2004), (in Polish).